Journal of Oceanography, Vol. 55, pp. 157 to 169. 1999

The Air-Sea Exchange of CO_2 in the East Sea (Japan Sea)

DONG-CHAN OH[1], MI-KYUNG PARK[1], SANG-HWA CHOI[2], DONG-JIN KANG[1], SUN YOUNG PARK[1], JEOM SHIK HWANG[1], ANDREY ANDREEV[3], GI HOON HONG[2] and KYUNG-RYUL KIM[1]

[1]*Department of Oceanography and Research Institute of Oceanography, Seoul National University, Seoul 151-742, Korea*
[2]*Korea Ocean Research & Development Institute, Ansan P.O. Box 29, Seoul 425-600, Korea*
[3]*Pacific Oceanological Institute, Russian Academy of Science, Vladivostok, Russia*

(Received 8 October 1998; in revised form 5 December 1998; accepted 10 December 1998)

During CREAMS expeditions, fCO_2 for surface waters was measured continuously along the cruise tracks. The fCO_2 in surface waters in summer varied in the range 320~440 μatm, showing moderate supersaturation with respect to atmospheric CO_2. In winter, however, fCO_2 showed under-saturation of CO_2 in most of the area, while varying in a much wider range from 180 to 520 μatm. Some very high fCO_2 values observed in the northern East Sea (Japan Sea) appeared to be associated with the intensive convection system developed in the area. A gas-exchange model was developed for describing the annual variation of fCO_2 and for estimating the annual flux of CO_2 at the air-sea interface. The model incorporated annual variations in SST, the thickness of the mixed layer, gas exchange associated with wind velocity, biological activity and atmospheric concentration of CO_2. The model shows that the East Sea releases CO_2 into the atmosphere from June to September, and absorbs CO_2 during the rest of the year, from October through May. The net annual CO_2 flux at the air-sea interface was estimated to be 0.032 (±0.012) Gt-C per year from the atmosphere into the East Sea. Water column chemistry shows penetration of CO_2 into the whole water column, supporting a short turnover time for deep waters in the East Sea.

Keywords:
- Surface fCO_2 in the East (Japan) Sea,
- air-sea CO_2 flux,
- seasonal variability of fCO_2,
- solubility pump,
- gas-exchange model.

1. Introduction

It is well known that the ocean plays a very important role in the overall biogeochemical cycle of CO_2 with its special pumping mechanisms such as solubility, biological, alkalinity and dynamic pumps (for the most recent summary, see IPCC, 1995). Thus, many studies on global changes in recent years have placed emphasis on quantifying these oceanic processes associated with CO_2 pumps.

The East Sea (Japan Sea) is one of the few ideal places for studying these oceanic processes on a regional scale. This is based on two facts that were confirmed during the recent CREAMS (Circulation Research of the East Asian Marginal Seas) Japan-Korea-Russia International cooperative studies on the East Sea:

(1) The East Sea has many open ocean characteristics such as a deep convection system, large seasonal variation in the sea surface temperature (SST) and comparable biological activities.

(2) The East Sea has undergone drastic changes in her ventilation system from the bottom water formation mode in the past to that of deep intermediate water formation at the present time (Kim and Kim, 1996). In particular, the change in the mode of ventilation system observed in the East Sea may resemble that which may be expected to occur in open oceans in the next century associated with recent global warming (Manabe and Stouffer, 1993). Therefore, understanding the carbonate system in the East Sea could provide very important clues to changes in global carbon cycles in the next century.

During the CREAMS expeditions, studies on CO_2 pumps in the East Sea were carried out. The studies included measuring parameters such as fugacity of CO_2 (fCO_2) in surface waters as well as in the atmosphere, and alkalinity and pH for the water column. In this paper, we report results mainly focused on the solubility pump operating at the air-sea interface of the East Sea. A simple model is devised to describe the annual variation of fCO_2 in surface waters. The net CO_2 flux at the air-sea interface is also estimated from the model.

2. Materials and Methods

Studies on the carbonate system were carried out 4 times during the CREAMS expeditions; twice on summer cruises, 95S and 96S, on board R/V Professor Khromov, and

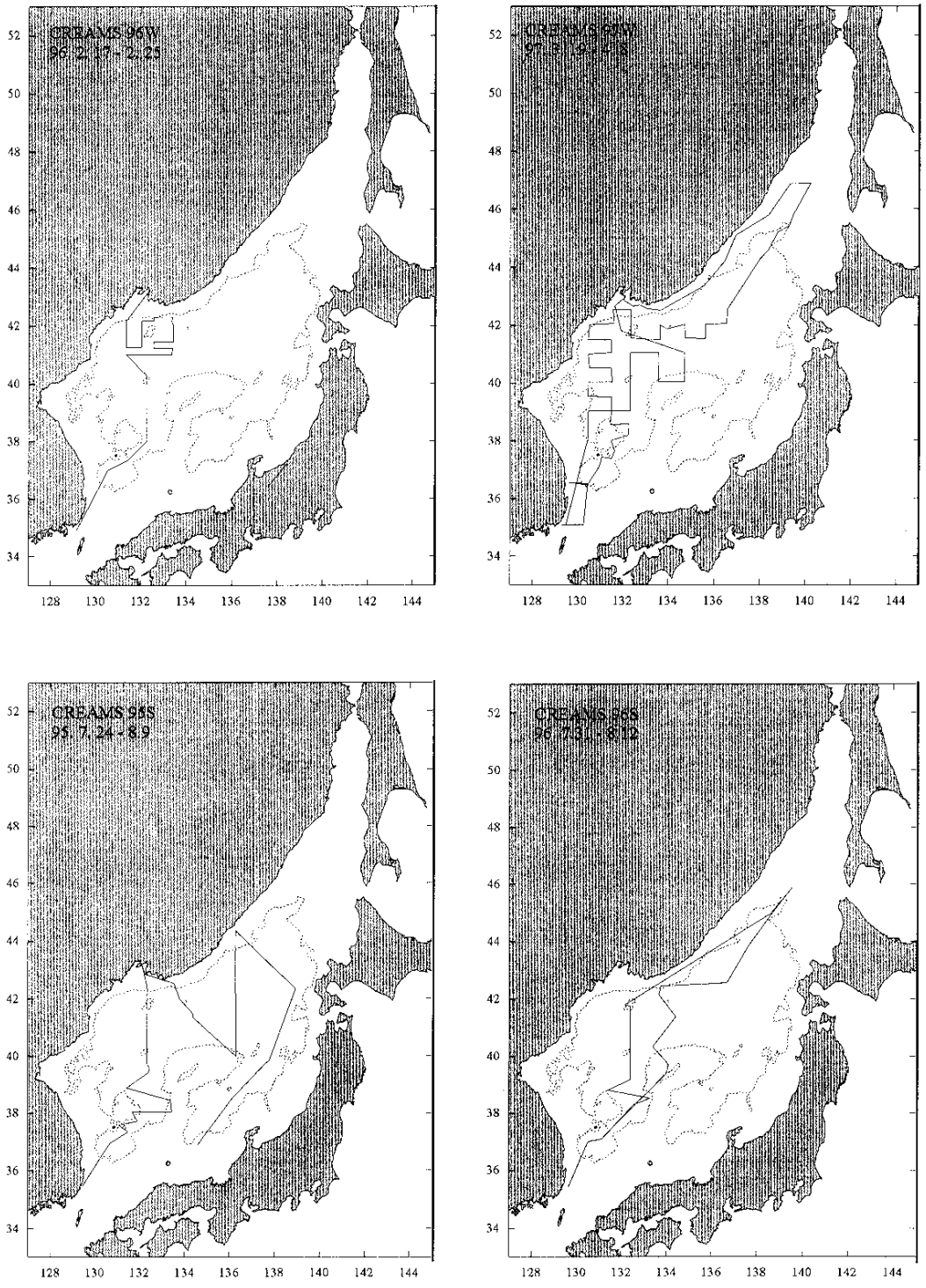

Fig. 1. Maps showing the cruise tracks of (a) CREAMS 96W in February 1996, (b) CREAMS 97W from March to April 1997, (c) CREAMS 95S from July to August 1995, and (d) CREAMS 96S expedition from July to August 1996. Dotted lines represent isopleth of 2000 m depth.

twice on winter cruises, 96W and 97W, on board R/V Parvel Gordienko. The cruise tracks of the four expeditions are shown in Fig. 1.

Partial pressures of CO_2 (pCO_2) in surface waters and air were measured continuously along the cruise track using a non-dispersive infrared CO_2 analyzer (NDIR; Licor-6252). Air was taken from an air intake tower mounted at the bow through the Dekabon tube (Dekoron, 3/8 inch) and surface waters were pumped up from the cooling system of the ship engines, which was located about 5 m below the sea surface. A Weiss-type equilibrator was used for the pCO_2 measurement of sea waters. pCO_2 was measured every second and was averaged over two-minute intervals. A schematic diagram for the overall analysis system is shown in Fig. 2.

SST and salinity of sea waters entering the equilibrator were measured with a thermosalinometer (Seabird SEACAT) every ten seconds. The temperature at the initial water intake was also measured continuously with a calibrated thermometer in order to correct for the warming effect during the flow through the tube from the intake to the equilibrator.

Along with the pCO_2 measurement, TA (Total Alkalinity) and pH of sea waters were determined regularly on board during the cruise. TA was determined by a potentiometric titration method (Millero *et al.*, 1993) and pH was measured spectrophotometrically (Clyton and Byrne, 1993). During the CREAMS 97W expedition, silicate and phosphate were also analyzed spectrophotometrically on board (Gordon *et al.*, 1993) along with TA and pH.

The fugacity of CO_2 in the moist equilibrator vapor, fCO_2, was calculated according to the algorithm by Weiss and Price (1980):

$$fCO_2 = pCO_2(P^{atm} - P^{sw})\exp[P^{atm}(B + 2\delta)/RT],$$

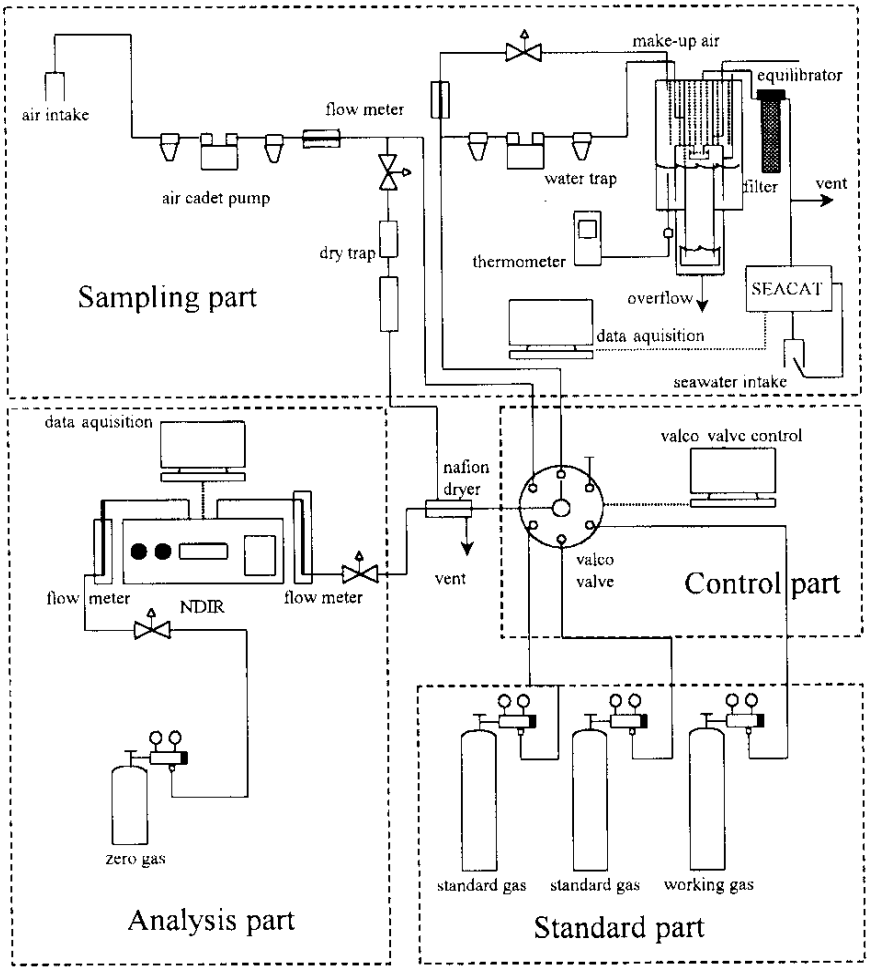

Fig. 2. Schematic diagram of CO_2 analysis system. pCO_2 is measured every second with an NDIR (non-dispersive infrared) CO_2 analyzer (Licor-6252). Temperature and salinity are measured every ten seconds with a thermosalinograph (SEACAT).

where pCO_2 is the partial pressure of CO_2 measured,

P^{atm} is the total barometric pressure in units of atmosphere,

P^{sw} is the saturated vapor pressure of sea water at the temperature of the measurements (Weiss and Price, 1980),

B and δ are the virial and cross-virial coefficients for CO_2, respectively (Weiss, 1974).

The *in situ* fugacity of CO_2 was calculated by correcting for the warming effect during the sea water flow from the intake to the equilibrator (~0.4°C) using the following equation (Weiss *et al.*, 1982):

$$\partial \ln fCO_2/\partial t = 0.03107 - 2.785 \times 10^{-4} t - 1.839 \times 10^{-3} \ln fCO_2,$$

where t is temperature in degrees Celsius.

3. Results

3.1 fCO_2 variations in surface waters

The fCO_2 variations in surface waters measured during the 4 cruises are shown in Fig. 3. The SST variations are also shown in the figure for comparison.

In summer, fCO_2 showed a variation with a range of 320~440 μatm, which was accompanied by a temperature variation from 15 to 28°C. The figures, especially during CREAMS 96S, clearly show that the variation of fCO_2 is quite parallel to that of SST, confirming the importance of temperature variation in controlling fCO_2 in surface sea waters (Peng *et al.*, 1987; Hirota *et al.*, 1991; Inoue *et al.*, 1995). The slope of the relative change in fCO_2 with respect to temperature, $\Delta fCO_2/fCO_2/\Delta T$, however, is 0.022~0.030 $°C^{-1}$, smaller than 0.042$°C^{-1}$ estimated with laboratory experiment by Peng *et al.* (1987), suggesting that other effects such as gas exchange and biological consumption processes are also important in the real situation.

In winter, fCO_2 showed much wider variations from ~200 μatm to ~520 μatm, with temperature changes from 0 to 15°C. While fCO_2 values in winter were low, i.e., below atmospheric values of around 360 μatm in most of the survey areas, some places in the northern East Sea showed high fCO_2 values, producing an apparent reverse trend between fCO_2 and SST (96W and early and later parts of 97W, in particular).

The process responsible for these high values can be understood by comparing fCO_2 with nutrients in surface waters as shown in Fig. 4. The observed data during 97W cruise clearly show that fCO_2 variation is similar to that of silicate and phosphate. The mixed-layer depths observed at several stations during the cruise were also linearly related to fCO_2 values at the stations, strongly implying that these high values of fCO_2 and nutrients originated from deep water

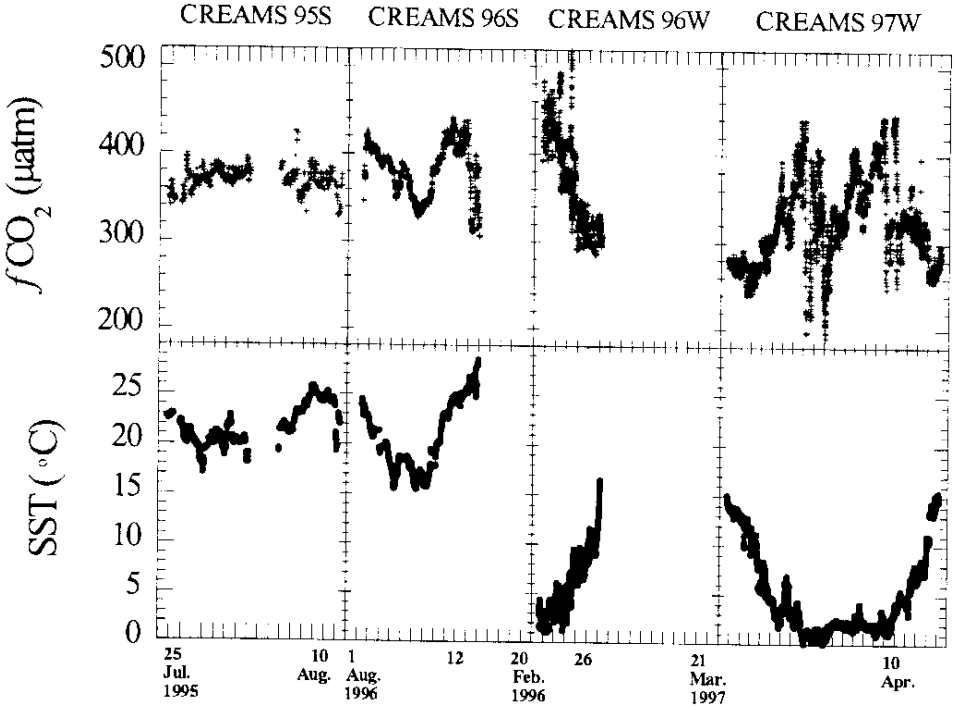

Fig. 3. Surface water fCO_2 and SST variations measured during 4 cruises, CREAMS 95S, CREAMS 96S, CREAMS 96W, and CREAMS 97W. Surface water fCO_2 varies in the range from 320 μatm to 420 μatm. The patterns of fCO_2 and SST variation are quite similar. SST seems to be the main parameter affecting surface water fCO_2.

brought to the surface through an intensive deep convection system developed in the area in winter time (Oh, 1998). Similar results were reported in the South Atlantic and Weddell Sea areas and in the western North Pacific (Takahashi *et al.*, 1993). The possibility of utilizing fCO_2 in surface waters as a surrogate for mixed-layer depths, thus locating areas of deep convection in the subpolar ocean in winter time, is further discussed elsewhere (Kim *et al.*, 1998).

3.2 ΔfCO_2 variations in surface waters

ΔfCO_2, defined as the difference between surface water fCO_2 and atmospheric fCO_2, ($fCO_2^{sw} - fCO_2^{air}$), represents the driving force for CO_2 exchanges at the air-sea interface. In Fig. 5, the distribution of ΔfCO_2 is shown, revealing that surface sea waters were, in general, supersaturated in summer with respect to atmospheric CO_2 and were undersaturated in winter time. Therefore, the East Sea serves as a source of atmospheric CO_2 in summer and as a sink in winter. However, notable exceptions are, of course, coastal areas with upwelling in summer, and deep convection areas in winter time.

4. Discussion

4.1 An air-sea interface gas-exchange model

A model was devised to describe the variation of fCO_2 in surface waters through time and to calculate the CO_2 flux at the air-sea interface. The model considered that the

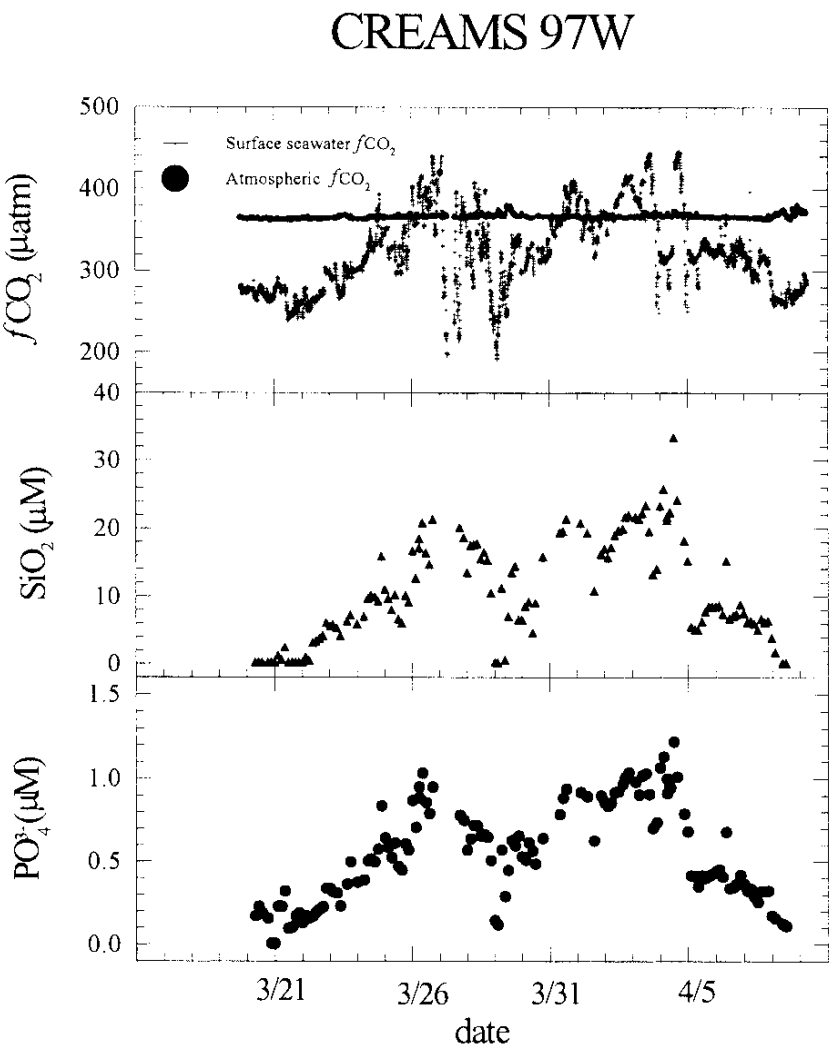

Fig. 4. Surface water fCO_2, silicate, and phosphate variations against time in CREAMS 97W expedition. The trends of surface water fCO_2 are opposite those of SST but quite similar to those of silicate and phosphate. This means that surface water fCO_2 is affected by vertical mixing with deep water which is relatively rich in CO_2 and nutrients.

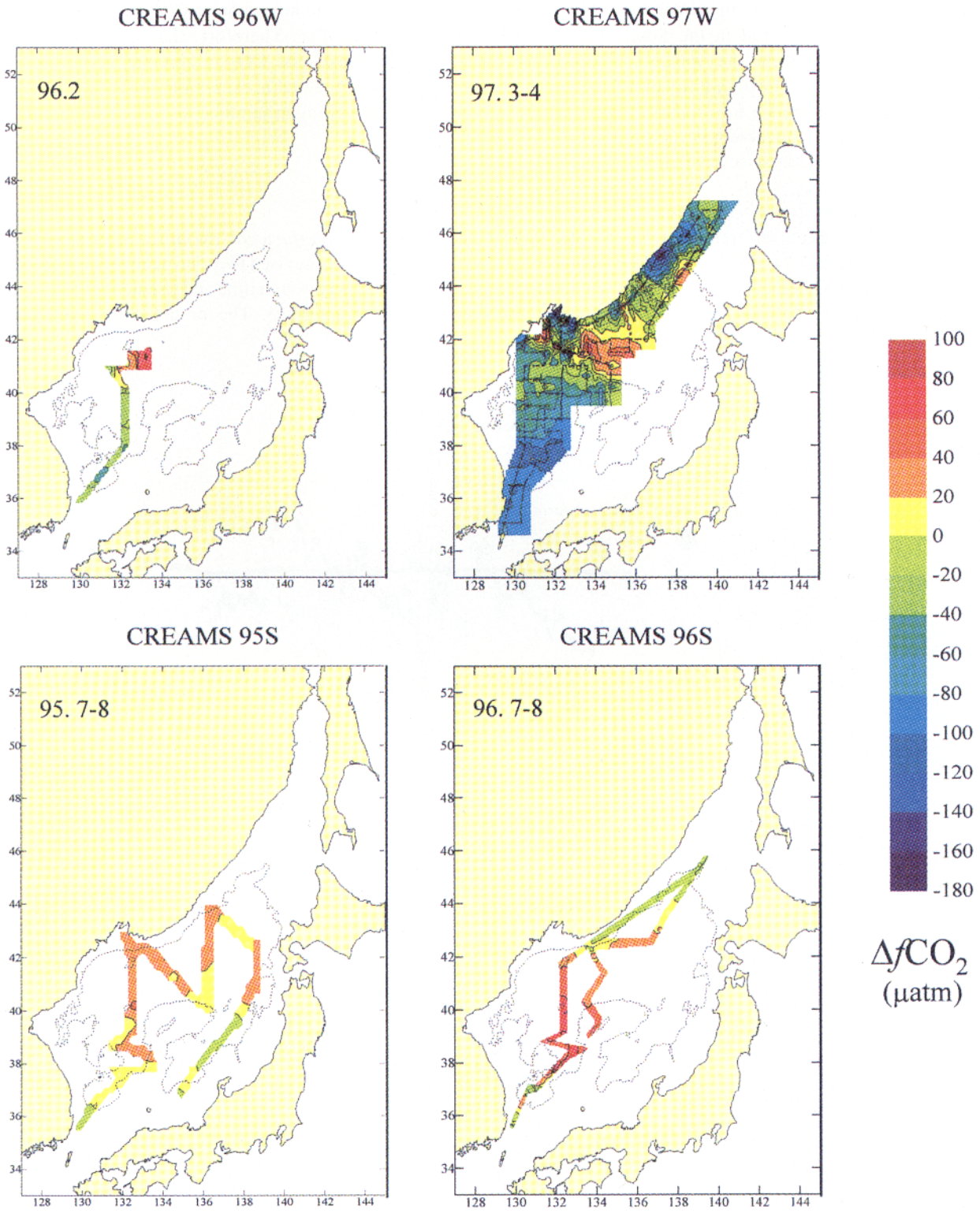

Fig. 5. The distributions of ΔfCO_2 ($fCO_{2seawater} - fCO_{2air}$) in the East Sea. They reveal that surface seawaters in the East Sea are, in general, supersaturated in summer and undersaturated in winter. In some areas in northern East Sea in winter time, however, high supersaturation of CO_2 was also observed, which could be due to intensive vertical mixing of upper waters.

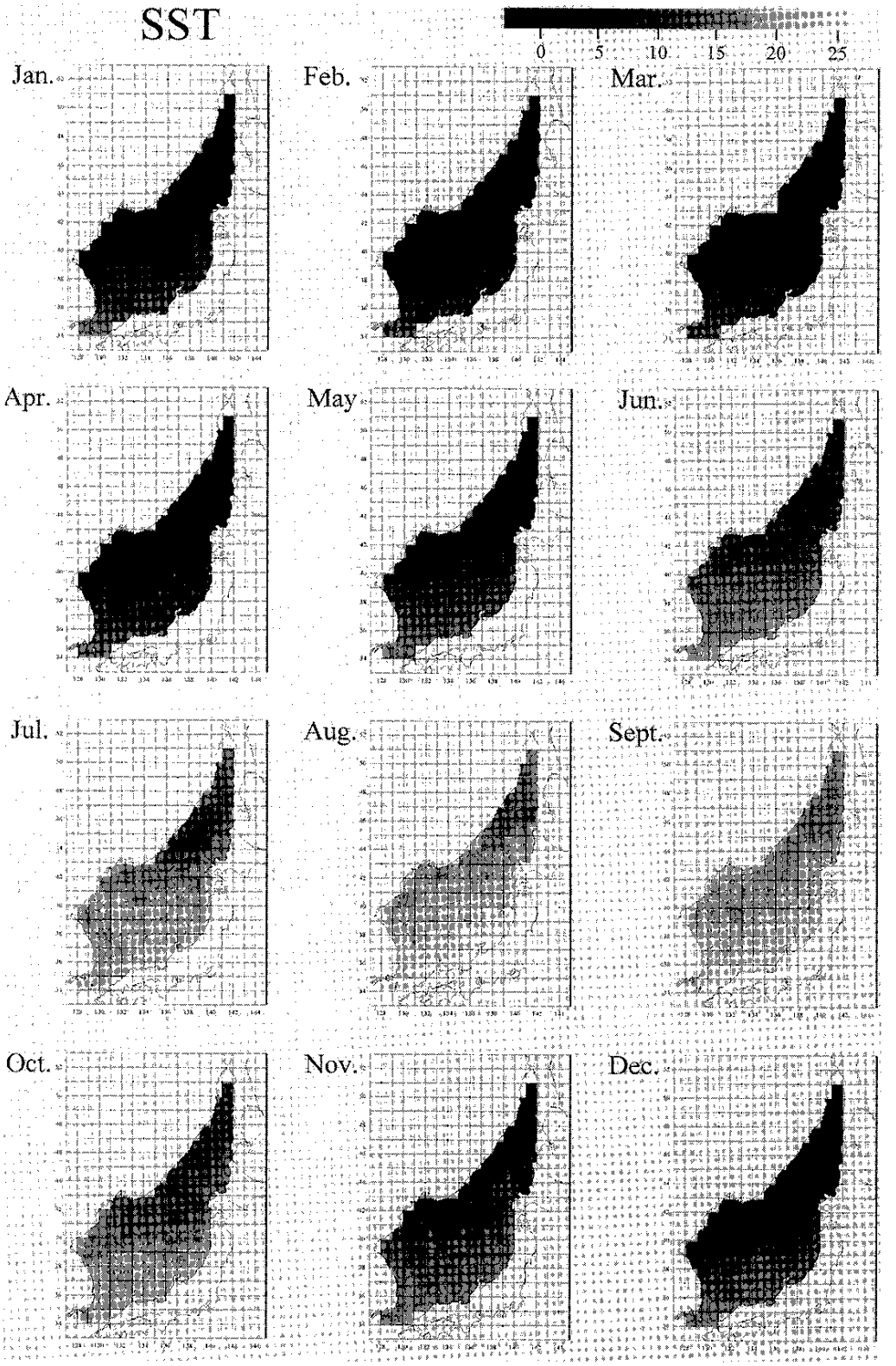

Fig. 6. Monthly mean SST in 1° × 1° grid in the East Sea. The East Sea can be divided into warm and cold regions with respect to SST. Even though the areas of warm and cold regions fluctuate seasonally, the boundary, which is a polar front, exists along the 40°N line except for coastal regions. The warm region represents subtropical waters whereas the cold region represents subpolar waters.

variation of surface fCO_2 in time resulted from the solubility pump associated with SST and salinity variation in time and gas exchange at the air-sea interface, the biological pump, and the dynamic pump, especially the change of mixed-layer depth with time.

4.1.1 Model parameters

For the model calculations, data for SST, mixed-layer depth (MLD), salinity, chlorophyll-*a*, wind velocity, and atmospheric fCO_2 were compiled for 111 grids (1° × 1° in size) as follows:

SST and salinity: The NODC (National Oceanographic Data Center) and JODC (Japan Oceanographic Data Center) databases containing data from 1932 to 1994 were used to calculate the monthly mean values for each grid.

MLD: MLD was defined as the depth with the maximum temperature gradient. MLD was estimated from temperature profiles obtained from the NODC CD-ROM listing data from 1932 to 1994.

Chlorophyll-a: CZCS chlorophyll-*a* data (Nimbus-7 satellite from 1978 to 1986) were used to estimate the characteristics of the biological pump. The biological production rate is estimated from the CZCS (Coastal Zone Color Scanner) chlorophyll concentration with an empirical CZCS chlorophyll—primary production relationship given by Smith and Baker (1977) as follows:

$$P^{eu} = 10^{[1.25+0.73\log\text{Chl-}a]},$$

where P^{eu} is the average production rate ($mg \cdot m^{-3} \cdot d^{-1}$) in the euphotic zone and Chl-*a* is the CZCS chlorophyll concentration ($mg \cdot m^{-3}$).

The depth of the euphotic zone was also calculated from chlorophyll-*a* data using the empirical relationship by Smith and Baker (1978):

$$Z^{eu} = 4.6[6.9 - 6.5\log\text{Chl-}a].$$

When the integrated biological activity for the whole surface mixed layer was estimated, Z^{eu} was used instead of MLD if Z^{eu} was shallower than MLD.

Wind speed: Diurnal wind speeds for every 1° by 1° grid were calculated with the Cardone Model based on diurnal weather maps (Na *et al.*, 1992); in model calculations actual wind data for 1993 were used. The gas transfer velocity (k_w) was estimated from the diurnal wind speed as follows (Wanninkhof, 1992):

$$k_w\ (m/s) = [2.5(0.5246 + 1.6256 \times 10^{-2}t + 4.9946 \times 10^{-4}t^2) + 0.3u^2](Sc/660)^{-1/2},$$

where t is SST (degrees in Celsius), u is the wind speed (m/s) at 10 m above the sea surface, and Sc is the Schmidt number.

The CO_2 flux at the air-sea interface was calculated as follows:

$$\text{Flux} = k_w\beta(fCO_2^{sw} - fCO_2^{air}) = k_w\beta(\Delta fCO_2),$$

where k_w is the gas transfer velocity and β is the solubility of CO_2.

Atmospheric fCO_2: Atmospheric fCO_2 is spatially constant in the East Sea area. The monthly average values from 1990 to 1996, monitored at the Kosan observatory on Cheju Island (Park, M.-K., 1997), were used in the model.

TCO_2: The depth dependence of TCO_2 was estimated from the average TCO_2 profile obtained in the Japan Basin during summer time.

The East Sea can be divided into two regions for model calculation: the northern ("cold region") shows typical characteristics for subpolar oceans, whereas the southern region ("warm region") is typical for subtropical oceans (Fig. 6; Kim and Kim, 1996). Therefore, the parameters estimated for each grid were averaged into two groups (cold region and warm region) as shown in Fig. 7, and were used for the model calculations. Except for wind velocity, all other parameters are monthly-average values and were fitted to smooth curves to give the daily variations.

4.1.2 Model algorithm

Figure 8 shows the algorithm for the model calculations. The procedure for model calculation is briefly summarized. It was assumed that total alkalinity (TA) is constant through time. The initial value is assumed to be 2307 $\mu mol\ kg^{-1}$ which is the average value calculated from actual observations at the East Sea during the cruises (Oh, 1998). With the initial TCO_2, fCO_2 in the air, SST, salinity, MLD and k_w as input, fCO_2 and pH in surface waters are calculated first and the daily CO_2 flux at the air-sea interface is assessed. Next, the integrated TCO_2 for the whole mixed layer of the day is calculated by multiplying TCO_2 by the mixed-layer depth (MLD);

$$\text{Integrated } TCO_2(d) = TCO_2(d) \times \text{MLD}(d).$$

Then, the integrated TCO_2 for the next day, Integrated $TCO_2(d+1)$, is calculated by subtracting the effects of the biological pump and gas exchange between the mixed layer and atmosphere as follows:

$$\text{Integrated } TCO_2(d+1) = \text{Integrated } TCO_2(d) - \text{Flux} - B,$$

where Flux represents the CO_2 flux derived from gas-exchange process at the air-sea interface ($mmole\ C \cdot m^{-2} \cdot d^{-1}$), and B is the rate of the biological pump ($mmole\ C \cdot m^{-2} \cdot d^{-1}$) which refers to the process by which export production removes carbon from the ocean surface layer to the ocean interior (Denman *et al.*, 1995). B is assumed to be 10% of the primary production in MLD (Broecker and Peng, 1982).

These procedures are repeated for 365 days and are then started all over again for the next year until the model produces stable results, which is usually achieved at the end of three years.

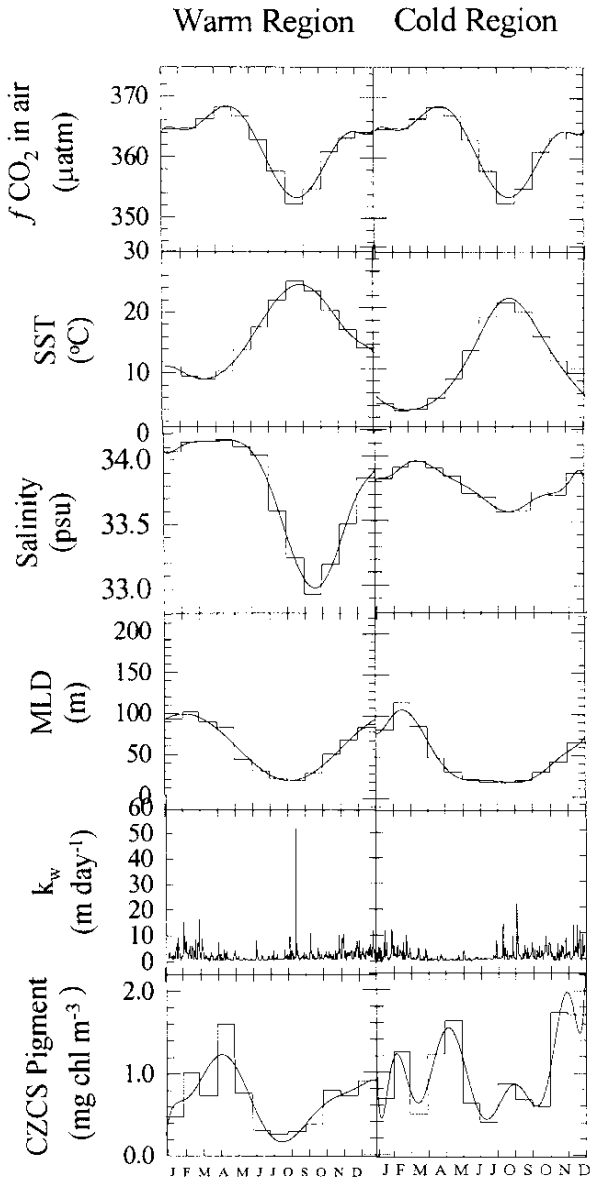

Fig. 7. Annual variation of parameters in the East Sea considered in this model. Due to differences in SST variations, the East Sea is divided into two regions (cold and warm regions) at 40°N in latitude.

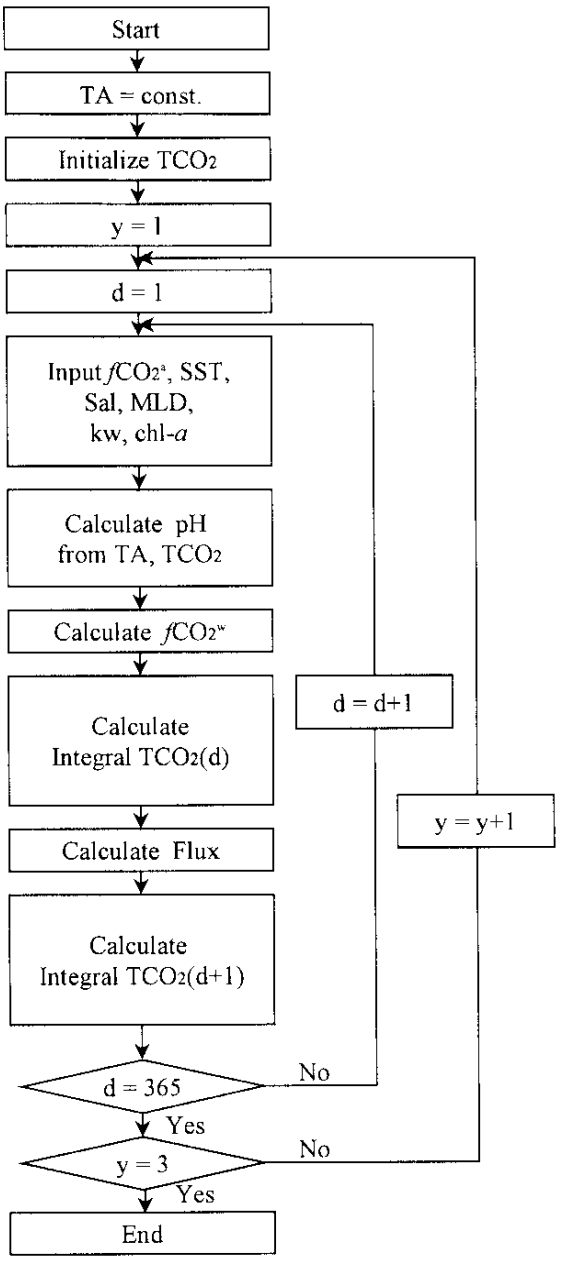

Fig. 8. The model algorithm for estimating surface water fCO_2 and flux at the-air sea interface through time.

4.1.3 Model results

Figure 9 shows the model results for warm regions and cold regions, clearly showing seasonal variation with higher values in summer and lower values in winter. The uncertainty of the model results can be estimated by running the model by varying the parameters within their own error limits (Oh, 1998). The uncertainty results mainly from the error for the rate of the biological pump. The uncertainty in fCO_2 is estimated to be ±60 μatm and is drawn as dashed curves in the figure.

The observed values during the CREAMS cruises are also shown as vertical lines in the figure. The agreement between the two sets of results is reasonably good. For the winter data, the range of anomalously high values due to the deep convection system is shown with dashed lines; this system could not be represented by the model for obvious reasons with moderate MLD in winter time.

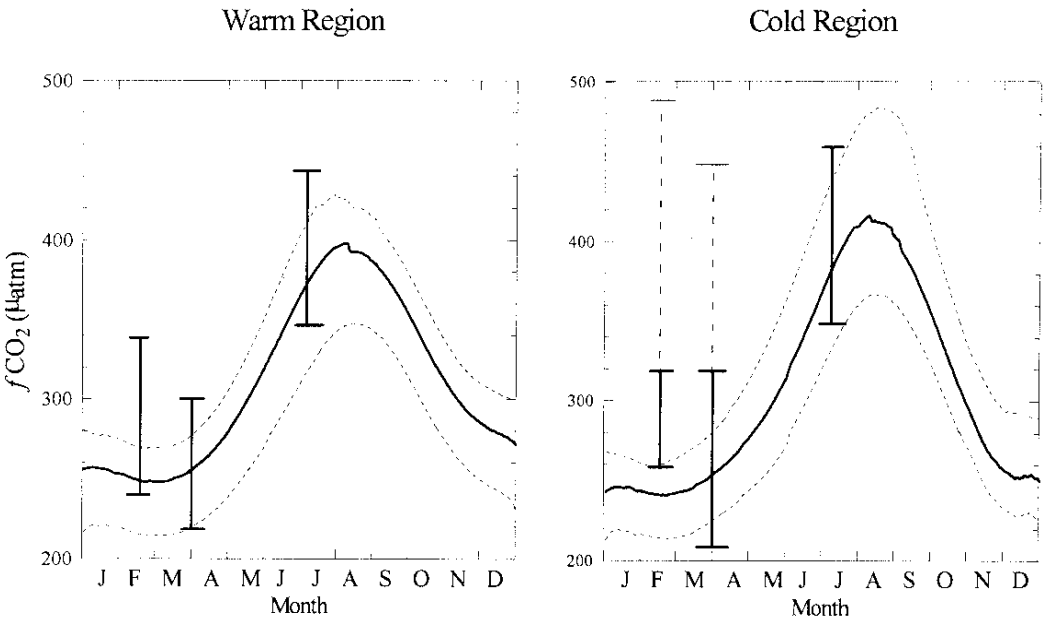

Fig. 9. The annual variation of fCO_2 estimated from the model in the East Sea. The values from our model are consistent with the observed ones in summer but there are some deviations in the cold region in winter.

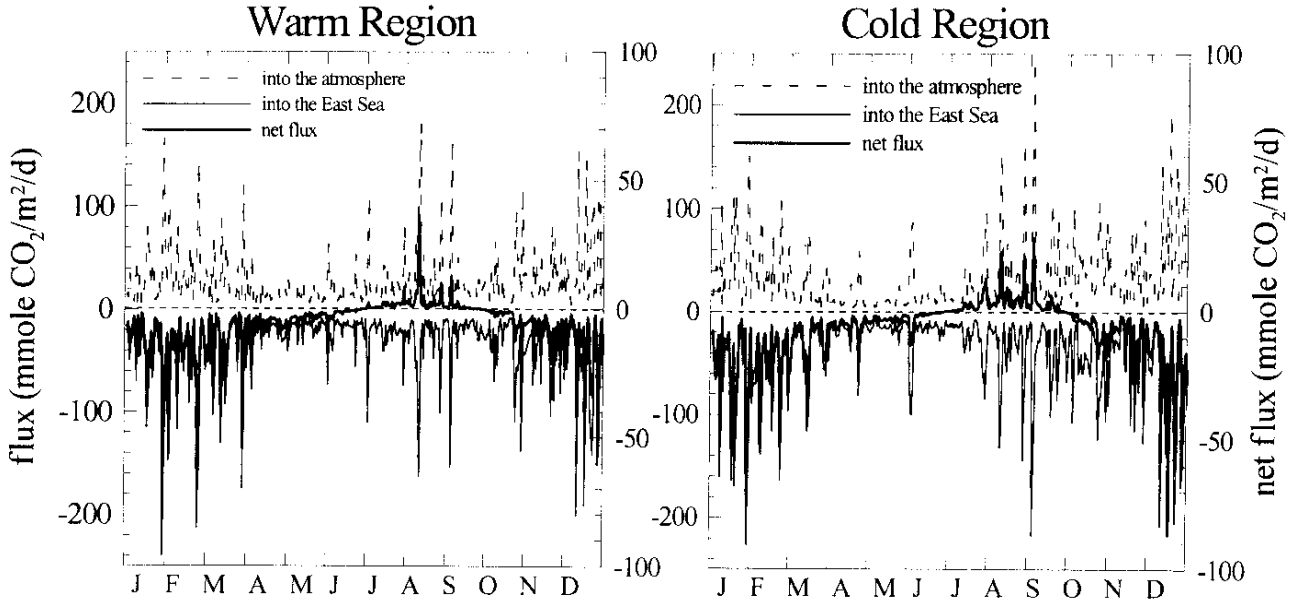

Fig. 10. The daily flux at the air-sea interface estimated from this model in the East Sea. There is a net flux from sea to air from July through September, and from air to sea from October to June. In general, gas exchanges are vigorous in winter but extremely high flux is predicted in summer due to typhoons.

4.2 CO_2 flux at the air-sea interface

From the model calculations, the daily flux of CO_2 at each region can be estimated and the results are given in Fig. 10. The net fluxes are much smaller than the real exchange fluxes and are shown on a different scale. The CO_2 exchange process at the air-sea interface is more intense in winter than in summer, except when a typhoon passes through the region. The model shows that there are net fluxes from the

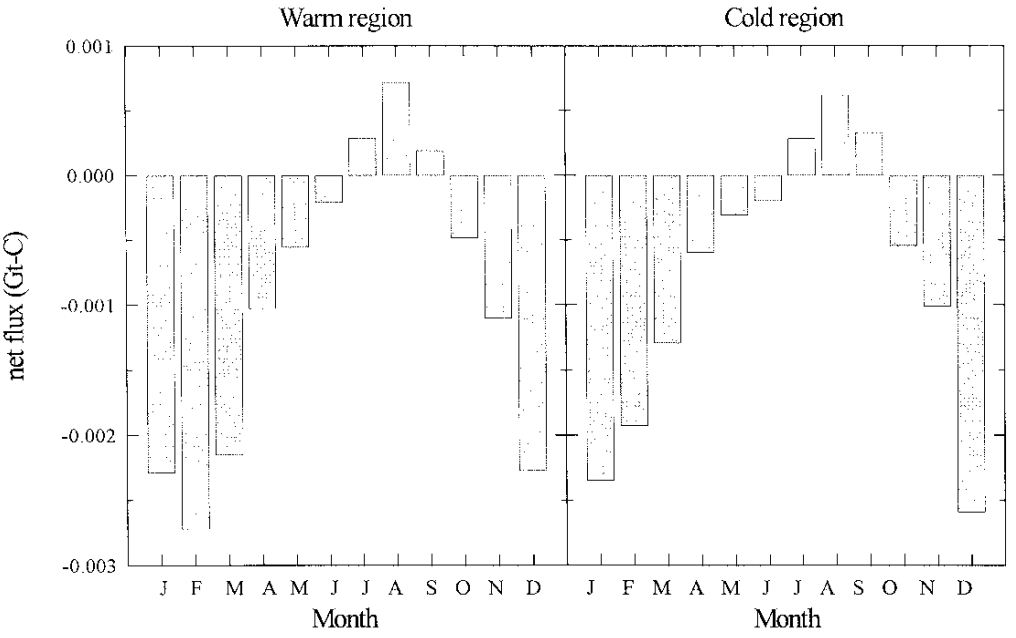

Fig. 11. Monthly integrated CO_2 fluxes at the air-sea interface for the warm and cold regions in the East Sea. A negative CO_2 flux means a CO_2 sink to the atmosphere and a positive value is a source to the atmosphere. The East Sea behaves as a CO_2 source in warmer months from July to September whereas it behaves a CO_2 sink in other seasons. The net CO_2 flux in the warm and cold regions is 0.014 (±0.005) Gt yr^{-1} and 0.018 (±0.007) Gt yr^{-1}, respectively.

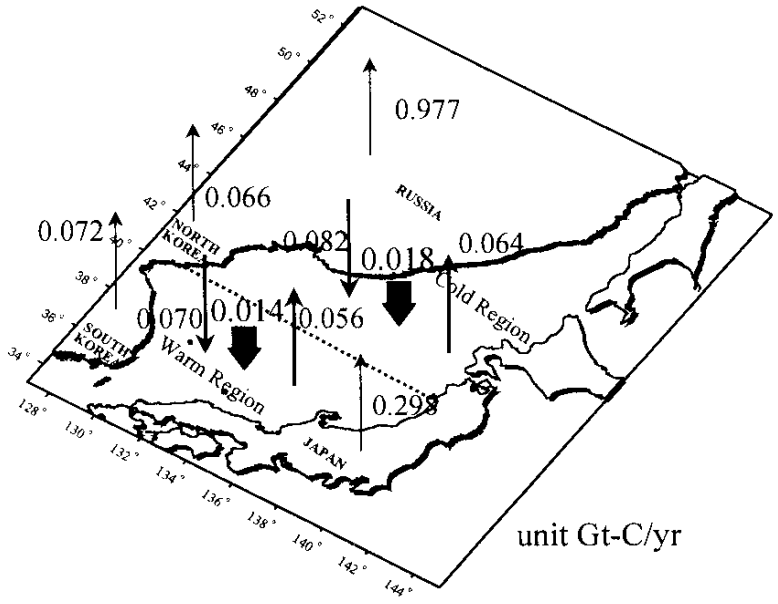

Fig. 12. The overall exchanges of CO_2 at the East Sea. The warm region absorbs 0.070 Gt-C and emits 0.056 Gt-C annually, resulting in a net absorption of 0.014 (± 0.005) Gt-C yr^{-1}. In the cold region, the East Sea emits 0.064 Gt-C and absorbs 0.082 Gt-C annually, producing an annual net absorption of 0.018 (± 0.007) Gt-C yr^{-1}. Anthropogenic emissions of CO_2 from nearby nations (Marland *et al.*, 1994) are also shown for comparison in the figure.

sea into the air in summer (from July to September) whereas these fluxes are from the air into the sea during the remaining period of the year (from October to May).

The monthly net flux is given in Fig. 11. The East Sea absorbs CO_2 from October to May, serving as an atmospheric CO_2 sink whereas it emits CO_2 from June through September, working as a CO_2 source. The warm region absorbs 0.070 Gt-C and emits 0.056 Gt-C annually, resulting in a net absorption of 0.014 (±0.005) Gt-C per year. In the cold region, the East Sea emits 0.064 Gt-C and absorbs 0.082 Gt-C annually, producing an annual net absorption of 0.018 (±0.007) Gt-C per year. Therefore, the East Sea appears to serve as a net sink for atmospheric CO_2 and the annual net flux is 0.032 (±0.012) Gt-C per year. The overall exchanges of CO_2 at the East Sea are summarized in Fig. 12. In the figure, anthropogenic emissions of CO_2 from nearby nations are also shown for comparison.

5. Conclusions

fCO_2 for surface waters was measured continuously along the cruise tracks 4 times during CREAMS expeditions. In summer, the fCO_2 in surface waters varied in the range 320~440 μatm, showing moderate supersaturation with respect to atmospheric CO_2. However, in winter, fCO_2 showed undersaturation of CO_2 in most of the area, while fCO_2 varied in a much wider range from 180 to 520 μatm. Some very high fCO_2 values, observed in northern East Sea, appear to be associated with the intensive convection system developed in the area.

An air-sea gas-exchange model was developed for describing the annual variation of fCO_2 and for estimating the annual flux of CO_2 at the air-sea interface. The model incorporated annual variations in SST, mixed-layer depth, gas exchange associated with wind velocity, biological activity, and atmospheric concentration of CO_2. The model shows that the East Sea emits CO_2 into the atmosphere from June to September, and absorbs CO_2 during the rest of the year, from October through May. The net annual CO_2 flux at the air-sea interface was estimated to be 0.032 (±0.012) Gt-C per year from the atmosphere into the East Sea. This amount corresponds to about 1.5% of the annual oceanic uptake of CO_2 (2.1 ± 0.8 Gt-C; Tans *et al.*, 1993), about 5 times the global average CO_2 uptake rate per unit area by ocean.

Studies on the carbonate system in the water column also show penetration of CO_2 all the way to the bottom within entire basins, supporting a rapid turnover time in the area (Tsunogai *et al.*, 1993; Kim and Kim, 1996; Kumamoto *et al.*, 1998). The East Sea appears to have 0.25 Gt-C of excess CO_2 already in deep waters (Park, S. Y., 1997), indicating rapid penetration of anthropogenic CO_2 at the present time, consistent with the present study. Studies on constructing overall CO_2 cycles in the East Sea are under way at the present time.

Acknowledgements

The authors would like to express their sincere appreciation to Prof. M. Takematsu of Kyushu University for his extraordinary leadership carrying out CREAMS expedition successfully. The enthusiasm of Prof. Jong-Hwan Yoon of Kyushu University and Prof. Kuh Kim of Seoul National University was also very essential for making CREAMS in action. The authors would also like to express their thanks to the Captains, officers, all crew members of R/V Professor Khromov and R/V Parvel Gordienko for their professionalism in supporting science at sea. Two reviewers also provided constructive comments for the manuscript. Dedication of colleagues, Jun Hak Ki, Doshik Hahm, and Saewung Kim at the laboratory, has been the most essential ingredient to make science and keep it in the highest standard as we hoped. Supports from Mr. Chickin and Ms. Pavlona from POI were of great help during the CREAMS 97W cruise. CO_2 measurements and data analysis were supported by "G7 program: Background monitoring of global atmospheric constituents change (1996–1998)", Ministry of Environment, Korea. Data collection at sea was supported by Basic Science Research Institute Program, Ministry of Education, Korea (BSRI-97-5406). Center for Ocean Circulation and Cycles supports the final manuscript preparation. This work was also supported by Korea Ocean Research & Development Institute (BSPN00304).

References

Broecker, W. S. and T.-H. Peng (1982): p. 149–150. In *Tracers in the Sea*. Eldigio Press, New York.

Clyton, T. and R. H. Byrne (1993): Spectrophotometric seawater pH measurements: total hydrogen ion concentration scale calibration of m-cresol purple and at-sea results. *Deep-Sea Res.*, **40**, 2115–2129.

Denman, K., E. Hofmann and H. Marchant (1995): Marine biotic responses to environmental change and feedbacks to climate. p. 485–516. In *Climate Change 1995*, ed. by J. T. Houghton, L. G. Meira Filho, B. A. Callender, N. Harris, A. Kattenberg and K. Maskell, Cambridge Univ. Press, New York, U.S.A.

Gordon, L. I., J. C. Jennings, Jr., A. A. Ross and J. M. Krest (1993): A suggested protocol for continuous flow automated analysis (phosphate, nitrate, nitrite, and silicic acid). WOCE Hydrographic Operations and Methods, WOCE Operations Manual, WHP Office Report 91-1.

Hirota, M., K. Nemoto, A. Murata and K. Fushimi (1991): Observation of carbon dioxide concentrations in air and surface sea water in the western North Pacific ocean. *The Oceanographical Magazine*, **41**, 19–28.

Inoue, H. Y., H. Matsueda, M. Ishii, K. Fushimi, M. Hirota, I. Asanuma and Y. Takasugi (1995): Long-term trend of the partial pressure of carbon dioxide (pCO_2) in surface waters of the western North Pacific, 1984–1993. *Tellus*, **47B**, 391–413.

IPCC (1995): *Climate Change: The Science of Climate Change*. Cambridge University Press, New York, 572 pp.

Kim, K.-R. and K. Kim (1996): What is happening in the East Sea (Japan Sea)? *J. Oceangr. Soc. Korea*, **31**, 164–172.

Kim, K.-R., D.-C. Oh, M.-K. Park and K. Kim (1998): Surface pCO_2 as a real time tracer for deep convection in water at subpolar oceans: a case of the East Sea (Japan Sea), (in preparation).

Kumamoto, Y., M. Yoneda, Y. Shibata, H. Kume, A. Tanaka, T. Uehiro and M. Morita (1998): Direct observation of the rapid turnover of the Japan Sea bottom water by means of AMS radiocarbon measurement. *Geophys. Res. Lett.*, **25**, 651–654.

Manabe, S. and R. J. Stouffer (1993): Century-scale effects of increased atmospheric CO_2 on the ocean-atmospheric system. *Nature*, **364**, 215–217.

Marland, G., R. J. Andres and T. A. Boden (1994): Global, regional, and national CO_2 emissions. p. 505–584. In *Trends '93: A Compendium of Data on Global Change*, ed. by T. A. Boden, D. P. Kaiser, R. J. Sepanski and F. W. Stoss, ORNL/CDIAC-65, Carbon Dioxide Information Analysis Center, Oak Ridge National Laboratory, Oak Ridge, Tenn., U.S.A.

Millero, F. J., J.-Z. Zhang, K. Lee and D. M. Campell (1993): Titration alkalinity of seawater. *Mar. Chem.*, **44**, 153–166.

Na, J.-Y., J.-W. Seo and S.-K. Han (1992): Monthly-mean sea surface winds over the adjacent seas of the Korea Peninsular. *J. Oceangr. Soc. Korea*, **27**, 1–10.

Oh, D.-C. (1998): A study on the characteristics of fCO_2 distributions and CO_2 flux at the air-sea interface in the seas around Korea. M.S. Thesis, Seoul National University, Seoul, 105 pp. (in Korean).

Park, M.-K. (1997): A study on the atmospheric CO_2 in Korea. M.S. Thesis, Seoul National University, Seoul, 105 pp. (in Korean).

Park, S. Y. (1997): A study on the carbon cycle in the deep waters of the East Sea. M.S. Thesis, Seoul National University, Seoul, 107 pp. (in Korean).

Peng, T.-H., T. Takahashi, W. S. Broecker and J. Olafsson (1987): Seasonal variability of carbon dioxide, nutrients and oxygen in the northern North Atlantic surface water: Observations and model. *Tellus*, **39B**, 439–458.

Smith, R. C. and K. S. Baker (1977): The bio-optical state of ocean waters and remote sensing. Scripps Institution of Oceanography Technical Report No. 77-2, San Diego, California, 35 pp.

Smith, R. C. and K. S. Baker (1978): The bio-optical state of ocean waters and remote sensing. *Limnol. Oceanogr.*, **23**, 247–259.

Takahashi, T., J. Olafsson, J. G. Goddard, D. W. Chipman and S. C. Sutherland (1993): Seasonal variation of CO_2 and nutrients in the high-latitude surface oceans: A comparative study. *Global Biogeochem. Cycles*, **7**, 843–878.

Tans, P., J. A. Berry and R. Keeling (1993): Oceanic $^{13}C/^{12}C$ observations: A new window on oceanic CO_2 uptake. *Global Biogeochem. Cycles*, **7**, 353–368.

Tsunogai, S., Y. W. Watanabe, K. Harada, S. Watanabe, S. Saito and M. Nakajima (1993): Dynamics of the Japan Sea deep water studied with chemical and radiochemical tracers. p. 105–119. In *Deep Ocean Circulation, Physical and Chemical Aspects*, ed. by T. Teramoto, Elsevier Sci. Pub., B.V.

Wanninkhof, R. (1992): Relationship between wind speed and gas exchange over the ocean. *J. Geophys. Res.*, **97**, 7373–7382.

Weiss, R. F. (1974): Carbon dioxide in water and seawater: the solubility of a non-ideal gas. *Mar. Chem.*, **2**, 203–215.

Weiss, R. F. and B. A. Price (1980): Nitrous oxide solubility in water and seawater. *Mar. Chem.*, **8**, 347–359.

Weiss, R. F., R. A. Jahnke and C. D. Keeling (1982): Seasonal effects of temperature and salinity on the partial pressure of CO_2 in seawater. *Nature*, **300**, 511–513.